Low-voltage resistance in small Josephson junctions

G Y Hu and R F O'Connell

Department of Physics and Astronomy, Louisiana State University, Baton Rouge, LA
70803-4001, USA

Abstract. Recent experiments by Iansiti *et al* on small Josephson junctions display
various novel features: a finite resistance R_0 associated with the low-voltage state, the
co-existence of Coulomb blockade and Josephson tunnelling, ... Since the existence
of R_0 cannot be explained by the simple RSJ model, nor by any classical model at
low-temperatures, we adopt a quantum Langevin equation approach which incorporates
frequency-dependent dissipation as well as dissipative quantum tunnelling. We obtain
good agreement between our theory and the results of Iansiti *et al* which reflects the
influence of the environment.

1. Introduction

Recently [1–4], new lithographic and low-temperature techniques have allowed the
fabrication and measurement of Josephson junctions with small areas for which the
Josephson coupling energy $E_J = \hbar I_c/2e$ (where I_c is the ideal critical current) is of
the order of the charging energy $E_c = e^2/2C_J$ (where C_J is the capacitance of the
junction). Several experimental studies of this type of junction have revealed a new
kind of current–voltage $(I–V)$ characteristic that exhibits both hysteresis and a small
voltage associated with the nominal zero-voltage branch [1–4]. This low-voltage state
can be characterized by a resistance R_0, which is not possible to explain within the
simplest classical model, the resistivity and capacitively shunted junction (RSJ) model,
which rules out the simultaneous presence of hysteresis and a low-voltage state in a
single $I–V$ curve [4]. Many theoretical efforts [1–4] have been made towards a full
understanding of this novel phenomenon.

Ono *et al* [1] have proposed that the coexistence of hysteresis and a low-voltage
state in a single $I–V$ curve can be explained either by an extended RSJ model where
the shunt conductance of the junction is frequency-dependent, or by a dissipative
quantum tunnelling model. Kautz and Martinis [4] (KM) have fully explored the
possibility of an extended RSJ model explanation by using models in which the
damping increases with frequency. In the KM model, the isolation resistor and lead
capacitance of the experimental apparatus are approximately accounted for by adding
R_s and C_b respectively to the RSJ circuits as shown in figure 1. Since the role
played by R_s and C_b in figure 1 is significant only in the high-frequency range, the
damping in the circuit is low at zero frequency and high at microwave frequency. The
analysis of KM is restricted to the *classical* regime ($E_J \gg E_c$) and their evaluation
of the finite resistance R_0 associated with the low-voltage state depended crucially
on the existence of thermal noise. Thus, in the low-temperature regime another

explanation is required. In particular, Iansiti *et al* [3] have explored the possibility of the dissipative quantum tunnelling model explanation and provided a semiquantitative account of their superconducting tunnel junction experiment in the low-temperature regime. Nevertheless, their explicit calculation of the resistance R_0 considered only the tunnelling rate in the absence of damping. Also, large discrepancies between the theory and experiments exists in the region where $E_J < E_c$. These studies [1–4] clearly established the basic physical elements associated with the low-voltage state in a small current-biased low-temperature Josephson junction: (i) dissipative quantum tunnelling plays an important role; (ii) the frequency-dependent damping behaviour brings the system originally thought to be in the weak-damping region into the strong-damping region. In this paper, we will first show that the frequency-dependent damping can be studied in the dissipative quantum tunnelling model, after which we calculate the $T = 0$ resistance R_0 in the presence of frequency damping by applying the KM model to the quantum regime.
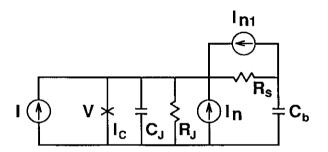

Figure 1. Josephson tunnelling junction in the Kautz and Martinis model, which is equivalent to an RSJ model with a frequency-dependent shunt.

The dissipative quantum tunnelling model [5–7] pioneered by Caldeira and Leggett (CL) is widely used in the literature and, with few exceptions [8], the path integral method is used to calculate the tunnelling rate. However, such a calculation is non-trivial, particularly in the case of frequency-dependent damping. Thus, various authors were motivated to present a new approach based on the use of the generalized quantum Langevin equation (GLE) [9–11]. The latter, which is derived from the same microscopic Hamiltonian used by CL and others, incorporates frequency-dependent damping by a frequency-dependent memory term. For a particle in a parabolic potential, Ford, Lewis and O'Connell (FLO) were able to obtain an exact result [9] and show, in agreement with CL, that dissipation always decreases the tunnelling rate (except in the presence of mass renormalization [10]).

While the GLE method is simpler to use than the path integral method (and it is particularly appealing for the problem at hand) the problem is that, so far, it is restricted to quadratic potentials. On the other hand, the CL method, has been applied to the cubic (more precisely, 'quadratic plus cubic') potential which is a good representation of the sinusoidal 'washboard' potential associated with the quantum tunnelling process in a current-biased Josephson junction provided that the external current I_{ext} is comparable to the critical current I_c.

2. Derivation of results

What we plan to do here is to combine the best features of both the CL and GLE approaches and obtain theoretical results with a single adjustable parameter. To explain what we have in mind we, first of all, review the case of weak coupling and ohmic damping since accurate results have been obtained by CL and others. At zero temperature, the decay rate from a metastable well is generally written as [5]

$$\Gamma = A \exp(-B/\hbar). \tag{1}$$

It is convenient to write

$$B = B_0 \Omega_0 / \Omega \equiv \beta B_0 \tag{2}$$

where Ω_0 and Ω are the small-oscillation frequencies at the local minimum of the potential, in the absence and presence of dissipation, respectively. In addition, for a current-biased Josephson junction in the cubic potential model, one has [5]

$$B_0 = \tfrac{36}{5} V_m / \Omega_0 \tag{3a}$$

where V_m, the barrier height, is given by [4]

$$V_m = 2E_J\{[1 - (I_{ext}/I_c)^2]^{1/2} - (I_{ext}/I_c)\cos^{-1}(I_{ext}/I_c)\}. \tag{3b}$$

Also for the *cubic potential* and in the case of *ohmic* damping, CL obtained

$$\Omega_0 / \Omega = 1 + b_1 \tag{4}$$

where

$$b_1 = [45\zeta(3)/2\pi^3]\gamma/\Omega_0 = 0.87(\gamma/\Omega_0) \tag{5}$$

represents the effect of dissipation to lowest order in γ, where γ corresponds to the damping parameter used by FLO [9]. For ease of comparison, we note that γ is twice the corresponding quantity used by CL and that the α used by these authors is our (γ/Ω_0). Finally, we refer to Freidkin *et al* [6] for an analysis of the effects of dissipation on A; the calculation is complicated and the result obtained is

$$A = \Omega_0(60B_0/2\pi\hbar)^{1/2}\exp(1.430\gamma/\Omega_0). \tag{6}$$

It is clear that the effects on the tunnelling rate due to dissipation term in A are much less important than those due to b_1.

The corresponding ohmic calculation in the case of the quadratic potential was carried out by FLO and these authors found a b_1 value equal to $(\gamma/2\Omega_0)$. It is thus clear that if we used an 'effective' coupling $\gamma_{eff} = 1.74\gamma$ in the quadratic calculation, we would conclude that the effects of dissipation, as given by b_1, are exactly the same as for the cubic calculation with a coupling constant γ. Another way of stating this (which will be useful when we turn to the non-ohmic problem) is that we replace β obtained from the quadratic calculation by β_{eff}. We conclude that the GLE method, originally designed for quadratic potentials is capable of treating the more complicated

cubic potential if we introduce a single adjustable parameter. This motivates us to use a similar approach in the more general case of non-ohmic dissipation and a more complicated potential (such as the 'washboard potential'). It should be emphasized that the cubic potential is only a good representation of the 'washboard potential' for $I_{ext} \simeq I_c$. However, the latter condition is not applicable in the present context (since the essence of the experiments under discussion is that I_{ext} is vanishingly small) and thus the path integral approach in its present development is not adequate. On the other hand, for our purposes, we will use the A and B_0 values associated with the cubic model (given, respectively, by equations (6) and (3a)) since Γ is only weakly dependent on the pre-factor A and also B_0 is multiplied by the adjustable parameter β.

We now turn to the non-ohmic problem. In the GLE approach, the presence of non-ohmic effects is reflected by the presence of a frequency-dependent memory function $\tilde{\mu}(\omega)$, which reduces to $m\gamma$ for ohmic dissipation, where m is a suitably defined 'mass' (see below). Thus, it is not unreasonable to calculate non-ohmic effects by carrying out the corresponding calculation for the quadratic model keeping in mind that we should replace β by β_{eff} at the end of the calculation (or, alternatively, regard β as an adjustable parameter) in order to make comparison with the experimental results. Whereas our approach does not give absolute numbers it should also be stressed that the experiments under discussion (in the non-ohmic regime) do not provide them either, in contrast to experiments carried out in the ohmic regime. However, an important test of our approach will be provided by the functional dependence of β on the environmental parameters (such as C_b and R_s appearing in (8) below). In fact we obtain an explicit analytic expression for this functional dependence (see equations (14) and (9) below).

The essence of the GLE approach is the calculation of (Ω_0/Ω) appearing in (2). This is achieved by solving the following equation (equations (17) of [9]):

$$[\alpha(i\Omega)]^{-1} \equiv m\Omega^2 + \Omega\tilde{\mu}(i\Omega) - m\Omega_0^2 = 0 \tag{7}$$

where $\tilde{\mu}(\omega)$ is the Fourier transform (denoted by a superposed tilde) of the memory function appearing in the GLE for the problem of interest and $\alpha(\omega)$ is the generalized susceptibility associated with the same GLE. Thus, in essence, our problem reduces to a determination of $\tilde{\mu}(\omega)$.

For the case of a Josephson junction, $m = \Phi_0^2 C_J$, where $\Phi_0 = \hbar/2e$ is the flux quantum, and also $m\Omega_0^2 = E_J [1 - (I_{ext}/I_c)^2]^{1/2}$, where I_{ext} is the external steady current and I_c is the critical Josephson current. For the RSJ model we have $\tilde{\mu}(\omega) = m\gamma$, where $\gamma = (C_J R_J)^{-1}$ and R_J is resistance of the junction i.e. we have ohmic dissipation. However, as already pointed out, this model is inadequate for our present purposes.

Since our goal is to calculate the finite resistance R_0 associated with the low-voltage state at low-temperature detected in the current-biased small Josephson junction, we will use the KM model which explains similar phenomenon quite well in the classical and finite temperature region. In the KM model, the isolation resistor and lead capacitance of the experimental apparatus, are modelled by the R_s and C_b respectively in the circuit shown in figure 1. Also I_n and I_{n1} refer to currents due to Johnson–Nyquist noise of the resistance R_J and R_s, respectively. Starting from the equation of motion (see equations (32) and (33) of [4]), it is straightforward to derive the GLE for the system, after which we obtain

$$\tilde{\mu}(\omega) = (\Phi_0^2/R_J)[(1 - i\omega C_b R_s R_J/R_{11})/(1 - i\omega C_b R_s)] \tag{8}$$

where $1/R_{11} = 1/R_s + 1/R_J$. The real part of $\bar{\mu}(\omega)$ was first obtained by KM in [4]. We next substitute (8) in (7) and obtain,

$$\Omega^3 + \alpha_s \eta \Omega_0 \Omega^2 + (\alpha_s \alpha_0 - 1)\Omega_0^2 \Omega - \alpha_s \Omega_0^3 = 0 \tag{9}$$

where

$$\alpha_0 \equiv (\Omega_0 R_J C_J)^{-1} = (\gamma/\Omega_0) \qquad \alpha_s = (\Omega_0 R_s C_b)^{-1} \qquad \eta = 1 + R_s R_{11}/C_b C_J. \tag{10}$$

Substituting the positive solution of (9) into (2), and using (1) and (6), we obtain the $T = 0$ quantum decay rate for the KM model in the weak damping ($\alpha_0 \ll 1$) limit

$$\Gamma = \Omega_0 (60 B_0/2\pi\hbar)^{1/2} e^{-B_0\beta/\hbar} \tag{11}$$

where $\beta \boxminus (\Omega_0/\Omega)$ is the positive solution of (9).

We are now in a position to apply the above-established dissipative quantum tunnelling theory to calculate the resistence R_0 associated with low-voltage state of the Josephson junction at $T \to 0$, and compare our theory with the experimental results of Iansiti *et al* [3].

It was first suggested by Ono *et al* [1] that the low-voltage state observed in their experiments corresponds to occassional quantum tunnelling, in which the phase slips by 2π with each tunnelling event and an average voltage appears across the junction given by $V_J = \pi\hbar\Gamma/e$, where Γ is the decay rate. It follows, that the resistance R_0 associated with this low-voltage state V_J is

$$R_0 = dV_J/dI_{ext}|_{I_{ext}=0} = (\pi\hbar/e)d\Gamma/dI_{ext}|_{I_{ext}=0}. \tag{12}$$

Based on this idea, Iansiti *et al* [3] calculated the R_0 in the absence of damping, which gives an upper bound of R_0 and provides a useful starting point. Here we apply the formalism developed in this paper to calculate the R_0 of (12) by means of the KM model where the damping is frequency-dependent.

Using (3) and (11), and after some algebra, we obtain from (12) an explicit expression for the tunnelling rate in the presence of damping

$$R_0 = h/e^2 (243\pi\hbar/10 B_0)^{1/2} [2B_0/\hbar\beta - 1] e^{-B_0/\hbar\beta} \tag{13}$$

where β is given by the solution of (9).

Some comments about (13) are in order. First of all, (13) demonstrates that after one includes the quantum tunnelling effect, the zero-voltage state originally appearing in the classical treatment of the Josephson junction is actually a low-voltage state with resistance R_0. In other words, the DC Josephson zero-voltage state is true only in the sense that for conventional samples $E_c \to 0$, $B_0/\hbar \gg 1$, and the tunnelling rate is negligibly small. Secondly, in the presence of current bias, the minimum of a potential well decreases consecutively along the forward direction of the current. Therefore, any backward tunnelling from the ground state is energetically unfavourable at $T = 0$. Equation (13) has included this fact and is a $T = 0$ forward tunnelling formula. Thirdly, damping plays a crucial role in obtaining (12) and (13) since it ensures that, after each tunnelling event, the phase falls into the local minimum before tunnelling again to give another 2π phase slip. Since we are working in the $I_{ext} \to 0$ limit, (13) is valid at any finite damping, which guarantees the dissipation of the energy gained by a 2π phase slip. Finally, (13) is a particularly convenient form for evaluating R_0 once β is known, as we will discuss in the following.

3. Comments

In general, the value of R_0 can be evaluated by first obtaining $\beta = \Omega_0/\Omega$ from (9) and then applying (13). The solution for the cubic algebra equation (9) is readily derived but it is lengthy and so will not be presented here. Instead, we discuss some of the special cases, which are of much physical interest. In the $R_s \to \infty$ limit, the effects of R_s and C_b can be neglected, and (8) and (9) reduce to the ohmic case [9], $\bar{\mu}(\omega) = \Phi_0^2/R_J$ and $\Omega^2 + \gamma\Omega = \Omega_0^2$, respectively. In that case, the normal mode frequency Ω is always close to Ω_0 in the weak damping region ($\gamma \ll \Omega_0$). When R_s becomes finite (in fact, $\alpha_s < 1$ in practice), even in the weak damping region, (9) has low-frequency solutions. In this case, one notices that η is the only quantity in (9) which is significantly larger than one, and (8) has an approximate solution

$$\beta \equiv \Omega_0/\Omega = \sqrt{\eta}(1 - 1(2\alpha_s\sqrt{\eta})). \tag{14}$$

For the KM model in the weak damping region ($\alpha_0 \ll 1$), we simply use (13) and (14) to calculate R_0. The results are illustrated in figure 2, where three different values of $\beta = 1$, 1.6, and 2.6 are used in the calculation (case $\beta = 1$ corresponds to the no damping situation). We recall that since we are in the weak damping region ($\gamma \ll \Omega_0$), large values of β (such as the 1.6 and 2.6 lines) only occur in cases where the environment plays a significant role. Two features of R_0 can be clearly identified by a comparison between the lines of different β in figure 2. First, at fixed value of β, R_0 decreases with decreasing E_c/E_J, and the rate of decrease is enhanced dramatically for $E_c/E_J \ll 1$. This implies that R_0 quickly becomes negligibly small when E_c/E_J drops to about 0.1. The second feature predicted by our theory is that at fixed E_c/E_J, R_0 decreases with increase of β, which reflects the fact that the frequency-dependent environmental damping reduces the tunnelling in our model.

For comparison, also shown in the figure, are the experimental data taken from [3]. These correspond to measurements on samples with different capacitances C_J and normal resistance R_J. The values of R_J for the four data points shown in figure 2 are, in increasing order of E_c/E_J, 14.8, 34, 70, and 110 (kΩ), respectively. The agreement between the theory and experiments is remarkable. As can be seen from the figure, when the junction capacitance C_J is relatively large ($E_c < E_J$) the experimental data basically fall into the range of the $\beta = 1$ theoretical curve. This suggests that when $E_c < E_J$ and $\gamma/\Omega_0 < 1$, the environment effect on the tunnelling is unimportant. On the other hand, when C_J is small ($E_c > E_J$), the $\beta = 1$ curve is far from the experimental data, which fall into the region where $\beta > 1$. In fact, one observes that the $\beta = 1.6$ and 2.6 curves fit the experimental data at about $E_c/E_J = 0.85$ and 5.0 respectively. This is really what one would expect: the smaller the C_J the larger the influence of the C_b and R_s from the external source. Thus we conclude that the discrepancy between the experimental data and the no-damping ($\beta = 1$) theory for the R_0 in the $E_c > E_J$ region can be solved once we take into account the damping effect of the environment (leads, etc). If we use the KM model and take a value $C_b/C_J = 15$ (a typical value used in [4]) to fit the data of [3], we conclude, from (14) and (10), that the values of $\beta = 1.6$ and 2.6 requires $R_s/R_J \approx 0.01$ and 0.001, to achieve a good fit to the experimental data for $R_J = 34$ kΩ, 110 kΩ respectively.

4. Conclusion

In summary, in this paper we have studied frequency-dependent dissipative quantum
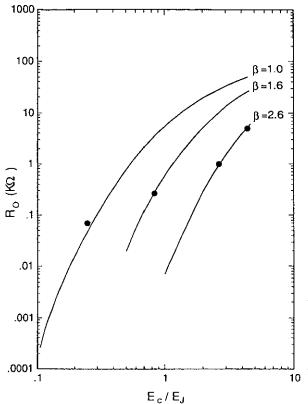
Figure 2. The zero temperature low-voltage resistance R_0 versus E_c/E_J (charging energy/Josephson energy) for a Josephson tunnelling junction. Full dots are experimental data taken from [3]. The solid lines are theoretical results calculated from equations (13) and (14) in the text, for three different values of $\beta \boxminus (\Omega_0/\Omega)$.

tunnelling by adopting the generalized quantum Langevin equation approach. By using the KM model for the frequency-dependent damping in the small Josephson tunnelling junction, we obtain the analytic expression (13) for the resistance R_0 associated with the low-voltage state at $T \to 0$. The theory fits the experimental data of Iansiti *et al* [3] very well and suggests that the experimentally measured value of R_0 in the $E_c > E_J$ region reflects the influence of the environment (leads, etc).

Finally, with a view toward outlining what we feel are key issues for further study, we recall previous detailed work on dissipative macroscopic quantum tunnelling. In particular, the review of Clarke and collaborators [12] points out the excellent agreement which has been obtained between experiments on Josephson tunnel junctions at low-temperatures and the theoretical work of Caldeira and Leggett [5]. Particularly impressive here is the fact that the parameters of the junction have been independently determined. On the other hand, these investigations were confined to the case of ohmic damping (corresponding to a Markovian interaction i.e. the absence of so-called memory effects) and an external current regime such that I_{ext} is comparable to I_c (so that the washboard potential could be substituted for the more complicated cubic potential).

By contrast, we note that in the experiments of Iansiti *et al* [2, 3] all the junction parameters are not known exactly. However, these experiments are exploring a new dimension viz. the realm of non-ohmic dissipation (corresponding to a non-Markovian interaction, reflecting the presence of memory effects) and a realm in which the cubic potential is not an adequate representation of the washboard potential. Whereas the

path integral method used by CL and others has also been applied by Esteve *et al* [13] to the case of a non-trivial memory function (describing the influence of a transmission line), these authors did not consider the more complicated potential relevant to the experiments presently under discussion. The method which we have presented here treats the problem at the expense of having a single adjustable parameter β. We see from figure 2 that whereas the $\beta = 1$ curve (no dissipation) is at variance with observations, the $\beta \neq 1$ curves can explain the observations and the curves with the larger β values correspond to the experimental samples displaying the largest dissipation.

Thus, there is a challenge to experimentalists to determine all the junction parameters independently in the non-ohmic case and there is a challenge to theorists to calculate numbers with no adjustable parameters. Since we believe that the latter endeavour is a non-trivial task using the method of [5], we decided to use a method based on a formula, equation (7) above, which is derived exactly from the generalized quantum Langevin equation in the case of a harmonic potential. The latter restriction means that we need to introduce one adjustable parameter but the advantage of our procedure is that we can treat arbitrary non-ohmic dissipative environments in a relatively simple manner.

Acknowledgments

References

[1]   Ono R H, Cromar M J, Kautz R, Soulen R J, Colwell J H and Fogle W E 1987 *IEEE Trans. Magn.* MAG-23 1670
[2]   Iansiti M, Johnson A T, Smith W F, Rogalla H, Lobb C J and Tinkham M 1987 *Phys. Rev. Lett.* 59 489
      Iansiti M, Johnson A T, Lobb C J and Tinkham M 1988 *Phys. Rev. Lett.* 60 2414
[3]   Iansiti M, Tinkham M, Johnson A T, Smith W F and Lobb C J 1989 *Phys. Rev.* B 39 6465
[4]   Kautz R L and Martinis J M 1990 *Phys. Rev.* B 42 9903
[5]   Caldeira A O and Leggett A J 1981 *Phys. Rev. Lett.* 46 211; 1983 *Ann. Phys., NY* 149 374
[6]   Freidkin E, Riseborough P S and Hänggi P 1988 *J. Phys. C: Solid State Phys.* 21 1543
[7]   Schmid A 1986 *Ann. Phys., NY* 170 333
[8]   Browne D A, Chow K S and Ambegokar V 1989 *Quantum Fluids and Solids-1989* ed G G Ihas and Y Takano (New York: AIP) p 39
[9]   Ford G W, Lewis J T and O'Connell R F 1988 *Phys. Lett.* 128A 29
[10] Ford G W, Lewis J T and O'Connell R F 1991 *Phys. Lett.* 158A 367
[11] Pollak E 1986 *Phys. Rev.* A 33 4244
      Grote R F and Hynes J T 1980 *J. Chem. Phys.* 73 2715
      Eckern U and Lehr W 1987 *Japan. J. Appl. Phys.* 26 1399 suppl. 26-3
[12] Clarke J, Cleland A N, Devoret M H, Esteve D and Martinis J M 1988 *Science* 239 992
[13] Esteve D, Martinis J M, Urbina C, Turlot E, Devoret M H, Grabert H and Linkwitz S 1989 *Phys. Scr.* 29 121